View Article Online / Journal Homepage / Table of Contents for this issue

DALTON
FULL PAPER

Dinuclear Cu^{II} and Ni^{II} complexes of 3-formylsalicylic acid oxime: *cis*/*trans* topology and extension of a *cis*-Cu^{II}_2 complex to a pentanuclear $Cu^{II}Cu^{II}Mn^{II}Cu^{II}Cu^{II}$ complex

Kazuhide Ikeda, Masaaki Ohba and Hisashi Ōkawa *

Department of Chemistry, Faculty of Science, Kyushu University, Hakozaki, Higashiku 6-10-1, Fukuoka 812-8581, Japan

Received 17th April 2001, Accepted 16th August 2001
First published as an Advance Article on the web 2nd October 2001

Published on 02 October 2001. Downloaded by University of York on 22/10/2014 15:44:31.

3-Formylsalicylic acid oxime (H_3L) formed the following dinuclear Cu^{II} and Ni^{II} complexes: $[Cu_2(HL)_2]\cdot 0.5H_2O$ (**1**), $Na[Cu_2(HL)(L)]\cdot 3H_2O$ (**2**) and $[Ni_2(HL)_2]\cdot 2.5H_2O$ (**3**). The structures of $Na[Cu_2(HL)(L)(H_2O)]$ (**2′**) and $[Ni_2(HL)_2(H_2O)_4]\cdot 8H_2O$ (**3′**) have been determined by X-ray crystallography. Complex **2** has a *cis* arrangement of the two ligands providing dissimilar $\{CuN_2O_2\}$ and $\{CuO_4\}$ chromophores sharing the two phenolic oxygen atoms. The N_2O_2 cavity has a hydrogen-bonded N–O · · · H · · · O–N linkage as the lateral chain, and the Cu in this site has a square-pyramidal geometry with a water molecule at the axial site. The Cu in the O_4 cavity has a planar geometry. Complex **3** has a *trans* configuration with respect to its two ligands and each Ni has a six-coordinate geometry with two water molecules at the axial sites. Complex **1** has a *trans* configuration based on its having a chemical formula and IR spectrum similar to **3**. The following interconversion among dinuclear Cu complexes has been established by pH adjustment: *trans*-$[Cu_2(HL)_2]$ (**1**) $\rightleftharpoons$ *cis*-$[Cu_2(HL)(L)]^-$ (**2**) $\rightleftharpoons$ *trans*-$[Cu_2(L)_2]^{2-}$ (water molecules are omitted). On the other hand, **3** showed the following interconversion: *trans*-$[Ni_2(HL)_2]$ (**3**) $\rightleftharpoons$ *trans*-$[Ni_2(L)_2]^{2-}$. The *cis* Cu2 complex **2** was reacted with Mn^{II} to afford $[Mn\{Cu_2(HL)(L)\}_2(H_2O)_4]\cdot H_2O\cdot 2DMF$ (**4**) that has a linear pentanuclear $Cu^{II}Cu^{II}Mn^{II}Cu^{II}Cu^{II}$ structure formed by the coordination of two molecules of **2** to a Mn^{II} through a carboxylate group.

Introduction

Metal-condensed compounds are currently the subject of many studies because of interest in their physicochemical properties and functions arising from the interaction or interplay of metal ions in close proximity. In order to provide metal-condensed compounds, 'complex ligands' having one or more sites capable of donating to another metal ion(s) are often used. Complex ligands with *cis* dioximate groups within the molecular framework are of particular interest[1–9] because the dioximate bridge is known as a good magnetic mediator between a pair of metal ions. For example, complete spin-coupling occurs at room temperature in dioximate-bridged trinuclear Cu^{II} complexes derived from bis(dimethylglyoximato)cuprate(II). Recent focus is placed on dinuclear and trinuclear complexes with *cis* dioximate groups as building blocks for providing metal-condensed systems. Typical examples are the extension of a dinuclear $Ni^{II}Ni^{II}$ complex to a tetranuclear $Fe^{III}Ni^{II}Ni^{II}Fe^{III}$ system,[7] extension of heterodinuclear $M_b^{II}M_c^{II}$ complexes to a trimetallic $M_a^{III}(M_b^{II}M_c^{II})$ system[8] and extension of a trinuclear $Cu^{II}Mn^{II}Cu^{II}$ complex to a polymeric $\{(Cu^{II}Mn^{II}Cu^{II})Mn^{II}\}_n$ system[9] through *cis*-dioximate bridges. In the polymeric compound a long-range magnetic ordering of $T_c = 5.5$ K has been confirmed.

In this context it is important to search simple dinuclear building blocks having a *cis* dioximate bridging group. 3-Formylsalicylic acid itself and Schiff bases with primary amines are known to afford dinuclear complexes of the $M_2(L)_2$ type with a *trans* arrangement of two ligands.[10,11] Analogous 3-formylsalicylic acid oxime (Chart 1, abbreviated as H_3L) is expected to show *cis*/*trans* topology in M_2L_2 type complexation, depending upon the absence or presence of an interaction between two oxime groups within a dinuclear molecule. In this work the following dinuclear Cu^{II} and Ni^{II} complexes have been derived from H_3L: $[Cu_2(HL)_2]\cdot 0.5H_2O$ (**1**), $Na[Cu_2(HL)(L)]\cdot 3H_2O$ (**2**) and $[Ni_2(HL)_2]\cdot 2.5H_2O$ (**3**). The *cis* arrangement of the two ligands in **2** and the *trans* arrangement in **3** have been proved by X-ray crystallography, and the following interconversion by pH has been established for the complexes: *trans*-$[Cu_2(HL)_2]$ (**1**) $\rightleftharpoons$ *cis*-$[Cu_2(HL)(L)]^-$ (**2**) $\rightleftharpoons$ *trans*-$[Cu_2(L)_2]^{2-}$ and *trans*-$[Ni_2(HL)_2]$ (**3**) $\rightleftharpoons$ *trans*-$[Ni_2(L)_2]^{2-}$ (water molecules are omitted). The reaction of **2** with Mn^{II} ions has afforded $[Mn\{Cu_2(HL)(L)\}_2]$ (**4**) whose structure is studied along with its magnetic properties.

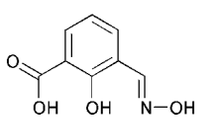

Chart 1 Chemical structure of H_3L.

Experimental

Physical measurements

Elemental analyses of carbon, hydrogen and nitrogen were obtained at The Service Center of Elemental Analysis of Kyushu University. Metal analyses were made on a Shimadzu AA-680 Atomic Absorption/Flame Emission Spectrophotometer. Infrared spectra were measured using KBr disks with a Perkin-Elmer Spectrum BX FT-IR system. Electronic absorption and reflectance spectra were recorded on a Shimadzu UV-3100PC Spectrophotometer. Magnetic susceptibilities of powdered samples were measured on a Quantum Design MPMS XL SQUID susceptometer in the temperature range 2–300 K. Diamagnetic corrections were made using Pascal's constants.[12]

Preparations

3-Hydroxyiminomethylsalicylic acid (H_3L). A mixture of an ethanol solution (150 cm^3) of 3-formylsalicylic acid[13] (1.66 g,

This journal is © The Royal Society of Chemistry 2001

View Article Online

Published on 02 October 2001. Downloaded by University of York on 22/10/2014 15:44:31.

10 mmol) and an aqueous solution (50 cm^3) of hydroxylamine hydrochloride (1.04 g, 15 mmol) were mixed and together with an aqueous solution (10 cm^3) of NaOH (0.60 g, 15 mmol) were refluxed for 5 hours and then evaporated to dryness. The residue was stirred with an aqueous $NaHCO_3$ solution (5%, 100 cm^3), and the aqueous extract separated from any insoluble material was neutralized with dilute hydrochloric acid to give a colorless precipitate. This was filtered off, thoroughly washed with water and dried *in vacuo*. The yield was 1.31 g (72%). Anal. Found: C, 52.15; H, 3.96; N, 7.67. Calcd for $C_8H_7NO_4$: C, 53.04; H, 3.90; N, 7.73%. IR [ν/cm^{-1}] as KBr disk: 3217, 1660, 1611, 1450, 1317, 1249, 1228, 1189, 957, 761, 681.

$[Cu_2(HL)_2]\cdot 0.5H_2O$ (1). A solution of H_3L (18 mg, 0.1 mmol) in dimethylformamide (DMF) (3 cm^3) was layered with a solution of copper(II) perchlorate hexahydrate (37 mg, 0.1 mmol) in water (2 cm^3) and allowed to stand at ambient temperature. After several days the resulting green microcrystals were separated, washed with diethyl ether and dried *in vacuo*. The yield was 21 mg (85%). Anal. Found: C, 38.69; H, 2.20; N, 5.82; Cu, 25.46. Calcd for $C_{16}Cu_2H_{11}N_2O_{8.5}$: C, 38.87; H, 2.24; N, 5.67; Cu, 25.71%. IR [ν/cm^{-1}] as KBr disk: 3367, 1600, 1573, 1432, 1360, 1267, 1230, 981, 883, 766, 696, 626. UV-vis [λ/nm (ε/M^{-1} cm^{-1})]: 657 [powder]; 628 (315) [in 0.1 M NaOH solution].

$Na[Cu_2(HL)(L)]\cdot 3H_2O$ (2). H_3L (181 mg, 1.0 mmol) was dissolved in an aqueous solution (100 cm^3) of NaOH (120 mg, 3.0 mmol). To this was added an aqueous solution of copper(II) acetate monohydrate (200 mg, 1 mmol), and the mixture was heated at reflux for one hour. The resulting green crystals were separated and recrystallized from an aqueous NaOH solution (0.4%, 100 cm^3). The yield was 160 mg (57%). Anal. Found: C, 34.11; H, 2.62; N, 4.97; Cu, 22.62. Calcd for $C_{16}Cu_2H_{15}N_2NaO_{11}$: C, 34.23; H, 2.69; H, 4.99; Cu, 22.64%. IR [ν/cm^{-1}] as KBr disk: 3488, 3076, 2998, 2923, 2853, 1607, 1586, 1430, 1348, 1269, 992, 754. UV-vis [λ/nm (ε/M^{-1} cm^{-1})]: 566 and 664 [powder]; 627 (320) [in 0.1 M NaOH solution].

$[Ni_2(HL)_2]\cdot 2.5H_2O$ (3). H_3L (181 mg, 1.0 mmol) was dissolved in an aqueous solution (100 cm^3) of NaOH (80 mg, 2.0 mmol). To this was added an aqueous solution (50 cm^3) of nickel(II) acetate tetrahydrate (248 mg, 1.0 mmol), and the mixture was allowed to stand for several days to afford $[Ni_2(HL)_2(H_2O)_4]\cdot 8H_2O$ (**3′**) as green crystals. Because they were highly efflorescent, elemental analyses were performed on the sample dried in air (**3**). The yield was 217 mg (83%). Anal. Found: C, 37.16; H, 2.78; N, 5.38; Ni, 22.14. Calcd for $C_{16}H_{15}N_2Ni_2O_{10.5}$: C, 36.91; H, 2.90; N, 5.38; Ni, 22.55%. IR [ν/cm^{-1}] as KBr disk: 3447, 3369, 1595, 1568, 1449, 1341, 1267, 1228, 968, 882, 762, 679, 621. UV-vis [λ/nm (ε/M^{-1} cm^{-1})]: 617 and 1120 [powder]; 620 (43) and 1137 (10) [in 0.1 M NaOH aq. solution].

$[Mn\{Cu_2(HL)(L)\}_2(H_2O)_4]\cdot H_2O\cdot 2DMF$ (4). To a solution of **2** (52 mg, 0.1 mmol) in a DMF–H_2O mixture (1 : 1 in volume, 60 cm^3) was added a solution of manganese(II) perchlorate hexahydrate (18 mg, 0.05 mmol) in DMF (10 cm^3), and the mixture was allowed to stand at ambient temperature forming green needles after a few days. The crystals were obtained as $[Mn\{Cu_2(HL)(L)\}_2(H_2O)_4]\cdot 4H_2O\cdot 2DMF$ (**4′**) based on X-ray crystallography as discussed later. In open air the compound loses three molecules of water to give $[Mn\{Cu_2(HL)(L)\}_2(H_2O)_4]\cdot H_2O\cdot 2DMF$ (**4**). The yield was 12 mg (19%). Anal. Found: C, 36.35; H, 3.35; N, 6.73; Cu, 19.96; Mn, 4.42. Calcd for $C_{38}Cu_4H_{42}MnN_6O_{23}$: C, 36.23; H, 3.36; N, 6.67; Cu, 20.17; Mn, 4.36%. IR [ν/cm^{-1}] as KBr disk: 3369, 1655, 1603, 1548, 1433, 1234, 994, 765. UV-vis [λ/nm]: 650 [powder].

X-Ray crystallography

A single crystal of $Na[Cu_2(HL)(L)(H_2O)]$ (**2′**) mounted on a glass fiber and a single crystal of $[Ni_2(HL)_2(H_2O)_4]\cdot 8H_2O$ (**3′**) sealed in a glass tube were used for X-ray crystallographic measurements using a Rigaku AFC7R diffractometer with graphite monochromated Mo-Kα radiation (λ = 0.71069 Å) and a 12 kW rotating anode generator. Cell constants and the orientation matrix for the data collection were obtained from 25 reflections and the ω–2θ scan mode was used for the intensity collections at 23 ± 1 °C. A single crystal of $[Mn\{Cu_2(HL)(L)\}_2(H_2O)_4]\cdot 4H_2O\cdot 2DMF$ (**4′**) was mounted on a glass fiber and used for crystallographic measurements using a Rigaku RAXIS-RAPID imaging plate area detector. Intensity data were collected by taking oscillation photographs. Pertinent crystallographic parameters for **2′**, **3′** and **4′** are summarized in Table 1)

The structures were solved by direct methods and expanded using Fourier techniques. The non-hydrogen atoms were refined anisotropically. Hydrogen atoms were included in the structure analysis but not refined. Computations were carried out on an IRIS O_2 computer using the TEXSAN crystallographic software package.[14]

CCDC reference numbers 162982–162984.

See http://www.rsc.org/suppdata/dt/b1/b103384k/ for crystallographic data in CIF or other electronic format.

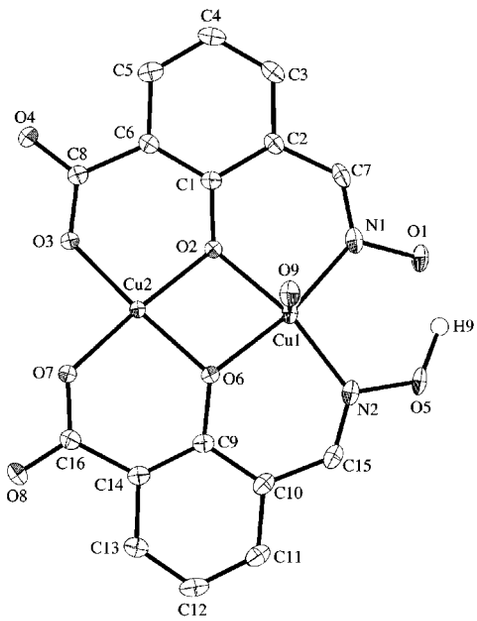

Fig. 1 An ORTEP view of $Na[Cu_2(HL)(L)(H_2O)]$ (**2′**) with the atom numbering scheme.

Results and discussion

Crystal structures

$Na[Cu_2(HL)(L)(H_2O)]$ (2′). An ORTEP[15] view of **2′** is shown in Fig. 1 together with the atom numbering scheme. Relevant bond distances and angles are given in Table 2.

The results clearly demonstrate the *cis* arrangement of the two ligands (HL^{2-} and L^{3-}) providing nonequivalent $\{CuN_2O_2\}$ and $\{CuO_4\}$ chromophores, sharing the two phenolic oxygen atoms. The Cu2···Cu1 interatomic separation is 2.961(1) Å. The N_2O_2 cavity has a hydrogen-bonded N1–O1···H···O5–N2 linkage formed by the dioximate group. The Cu1 in the N_2O_2 site has a square-pyramidal geometry with a water molecule at the apical site. The basal Cu-to-donor bond distances range from 1.943(3) to 1.958(2) Å. The axial Cu–O9 bond distance (2.378(2) Å) is elongated due to the Jahn–Teller effect of a d^9 electronic configuration. The O1···O5 separation (2.444(3) Å) is very short relative to the O···O separation (2.53–2.70 Å) of bis(dimethylglyoximato)copper(II)

View Article Online

Published on 02 October 2001. Downloaded by University of York on 22/10/2014 15:44:31.

Table 1 Crystallographic parameters for $Na[Cu_2(HL)L(H_2O)]$ (**2′**), $[Ni_2(HL)_2(H_2O)_4]\cdot 8H_2O$ (**3′**) and $[Mn\{Cu_2(HL)(L)\}_2(H_2O)_4]\cdot 4H_2O\cdot 2DMF$ (**4′**)

	2′	**3′**	**4′**
Empirical formula	$C_{16}H_{11}N_2Cu_2NaO_9$	$C_{16}H_{34}N_2Ni_2O_{20}$	$C_{38}H_{48}N_6Cu_4MnO_{26}$
Formula weight	523.35	691.85	1313.94
Crystal color	Green	Green	Green
Crystal system	Triclinic	Monoclinic	Triclinic
Space group	$P\bar{1}$ (no. 2)	$P2_1/a$ (no. 14)	$P\bar{1}$ (no. 2)
a/Å	9.347(3)	7.779(4)	11.2151(7)
b/Å	11.033(2)	15.561(4)	13.1298(7)
c/Å	8.607(2)	11.124(2)	8.2073(4)
α/°	101.65(2)	90.00	94.744(2)
β/°	92.07(2)	99.07(2)	99.760(2)
γ/°	75.28(2)	90.00	77.517(3)
V/Å^3	870.7(4)	1329.7(7)	1161.6(1)
Z	2	2	1
T/K	296	296	183
D_{calc}/g cm^{-3}	2.075	1.728	1.878
μ(Mo-Kα)/cm^{-1}	26.17	15.09	21.67
No. observations ($I > 3.00\ \sigma(I)$)	3258	2379	3506
R^a	0.034	0.033	0.033
R_w	0.058^b	0.056^b	0.046^c
G.O.F.	1.17	1.08	1.00

^{a} $R = \Sigma||F_o| - |F_c||/\Sigma|F_o|$. ^{b} $R_w = [(\Sigma w\,(|F_o| - |F_c|)^2/\Sigma wF_o^2)]^{1/2}$. ^{c} $R_w = [(\Sigma w\,(F_o^2 - F_c^2)^2/\Sigma w\,(F_o^2)^2)]^{1/2}$, $w = 1/[\sigma^2(F_o)] = [\sigma^2 c(F_o) + p^2F_o^2/4]^{-1}$.

Table 2 Selected bond distances (Å) and angles (°) for **2′**

Cu(1)–O(2)	1.958(2)	Cu(2)–O(2)	1.900(2)
Cu(1)–O(6)	1.955(2)	Cu(2)–O(3)	1.883(2)
Cu(1)–N(1)	1.943(3)	Cu(2)–O(6)	1.916(2)
Cu(1)–N(2)	1.947(2)	Cu(2)–O(7)	1.889(2)
Cu(1)–O(9)	2.378(2)	Cu(1)···Cu(2)	2.961(1)
O(2)–Cu(1)–O(6)	78.74(8)	O(2)–Cu(2)–O(3)	95.71(8)
O(2)–Cu(1)–N(1)	89.65(9)	O(2)–Cu(2)–O(6)	81.16(9)
O(6)–Cu(1)–N(2)	90.06(9)	O(3)–Cu(2)–O(7)	88.51(9)
N(1)–Cu(1)–N(2)	100.2(1)	O(6)–Cu(2)–O(7)	94.50(9)
Cu(1)–O(2)–Cu(2)	100.24(9)	Cu(1)–O(6)–Cu(2)	99.79(9)

$[Cu(Hdmg)_2]$[16] and is similar to that (2.44 Å) of $[Ni(Hdmg)_2]$.[17] This fact indicates strong hydrogen bonding in the N1–O1···H9···O5–N2 linkage. The O1–H9 and H9–O5 separations are 1.385(2) and 1.210(2) Å, respectively. The Cu2 in the O_4 site has a planar configuration with significantly short Cu2-to-donor bond distances (1.883(2)–1.916(2) Å). The molecule except for the aqua ligand forms a good co-plane. The axial aqua molecule is hydrogen-bonded to the carboxylate oxygen O8′ of an adjacent molecule.

$[Ni_2(HL)_2(H_2O)_4]\cdot 8H_2O$ (3′). An ORTEP drawing of **3′** is given in Fig. 2 together with the atom numbering scheme. Selected bond distances and angles are given in Table 3.

The molecule has a dinuclear core with a *trans* arrangement of the two HL^{2-} ligands. There exists an inversion center at the center of the four-membered ring formed by the two Ni atoms and the two phenolic oxygen atoms. Four of the twelve water molecules are involved in axial donation to the Ni ions, providing a pseudo octahedral environment about each Ni. The in-plane Ni-to-donor bond distances range from 2.005(2) to 2.035(2) Å. The axial Ni–O bond distances are slightly longer (2.075(2) and 2.130(2) Å). The Ni···Ni* interatomic distance is 3.031(1) Å and the Ni–O2–Ni* angle is 96.81(7)°. The two basal $\{NiNO_3\}$ planes are coplanar but the two $(HL)^-$ ligands are bent at the N1–O2–O3 edge with a dihedral angle of 32.94(8)°. Because of this bending, the bridging phenolic oxygen O2 shows a non-planar configuration. That is, the sum of the angles C1–O2–Ni, C1–O2–Ni* and Ni–O2–Ni* (345.3°) is significantly smaller than 360°.

Six water molecules in the lattice are hydrogen-bonded to the complex molecule through the oxime hydrogen atom H4 (H4*) (O1···O 2.705(4) Å), the carboxylate oxygen atom O4 (O4*) (O4···O 2.819(3) Å), and the hydrogen attached to O6 (O6*) (O6···O: 2.819(3) Å). The remaining water molecules are captured in the crystal lattice.

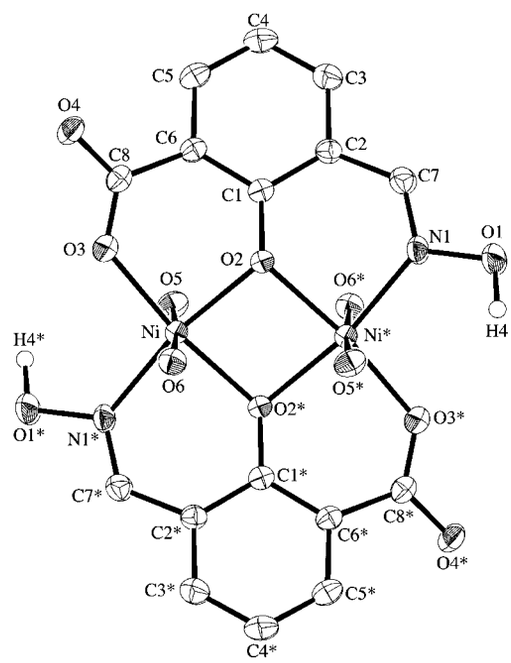

Fig. 2 An ORTEP view of $[Ni_2(HL)_2(H_2O)_4]\cdot 8H_2O$ (**3′**) with the atom numbering scheme.

Table 3 Selected bond distances (Å) and angles (°) for **3′**

Ni(1)–O(2)	2.018(2)	Ni(1)–O(5)	2.075(2)
Ni(1)–O(2*)	2.035(2)	Ni(1)–O(6)	2.130(2)
Ni(1)–O(3)	2.005(2)	Ni(1)–N(1)	2.031(2)
Ni(1)···Ni(1*)	3.031(1)		
O(2)–Ni(1)–O(3)	88.82(7)	O(2)–Ni(1)–N(1)	86.65(9)
O(2)–Ni(1)–O(5)	92.71(8)	O(3)–Ni(1)–O(5)	89.89(8)
O(2)–Ni(1)–O(6)	90.82(8)	O(3)–Ni(1)–O(6)	88.41(8)
O(2*)–Ni(1)–O(5)	90.38(8)	O(3)–Ni(1)–N(1*)	101.33(9)
O(2*)–Ni(1)–O(6)	91.80(7)	O(5)–Ni(1)–N(1*)	90.43(9)
O(2)–Ni(1)–O(2*)	83.19(7)	O(6)–Ni(1)–N(1*)	86.41(9)
Ni(1)–O(2)–Ni(1*)	96.81(7)		

Symmetry operation: $*-x, -y, -z$.

View Article Online

Published on 02 October 2001. Downloaded by University of York on 22/10/2014 15:44:31.

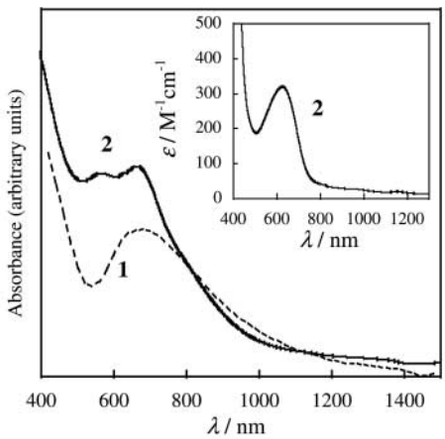

Fig. 3 Reflectance spectra of **1** and **2**. The insert is the absorption spectrum of **2** in 0.1 M NaOH solution.

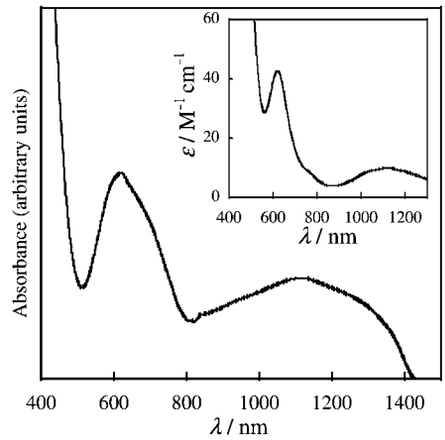

Fig. 4 Reflectance and absorption (in 0.1 M NaOH solution – insert) spectra of **3**.

It is interesting to compare the bite angles about the imine nitrogen N1 in compounds **2′** and **3′**. The C7–N1–Cu1, C7–N1–O1 and Cu1–N1–O1 angles for **2′** are 125.8, 116.0 and 118.2°, respectively, and the corresponding angles for **3′** are 124.1, 111.4 and 123.5°, respectively. It is seen that the C7–N1–O1 angle in **2′** is large relative to that in **3′** whereas the Cu1–N1–O1 angle in 2′ is small relative to that in **3′**. This fact adds support to the theory of strong hydrogen bonding in the N1–O1 · · · H9 · · · O5–N2 linkage in **2′**.

cis/*trans* Topology

The X-ray crystallographic studies have clearly demonstrated that **2** has a *cis* configuration whereas **3** has a *trans* configuration with respect to the arrangement of the two ligands. Complex **2** shows a sharp IR band at 2853 cm^{-1} that is attributable to the ν(OH) mode of a coordinated aqua molecule. A hydrogen-bonded dioximate group (N–O · · · H · · · O–N) generally shows a ν(OH) band at low frequency,[18] however, **2** shows no IR band attributable to an oxime group in the region 2000–1630 cm^{-1}. The oxime vibration can be located at lower frequency (< 1630 cm^{-1}) but is concealed by strong ligand IR bands. Complex **3** shows two sharp IR bands at 3447 and 3369 cm^{-1} superimposed on a broad band (3300–3500 cm^{-1}) due to lattice water. The former band can be assigned to the ν(OH) mode of a coordinated water molecule and the latter band to the ν(OH) mode of an oxime group. Complex **1** certainly has a *trans* configuration judging from its chemical formula (HL^{2-} : Cu = 2 : 2) and IR spectrum showing the ν(OH) band of an oxime group at 3367 cm^{-1}.

Complexes **1** and **3** are insoluble in water and **2** is sparingly soluble in water. The reflectance spectrum of **1** exhibits one d–d band at 657 nm (Fig. 3), whereas that of **2** has two d–d bands at 566 and 664 nm in accord with the non-equivalence about the two Cu^{II} ions. The reflectance spectrum of **3** has two bands at 617 and 1120 nm that can be assigned to the $^3T_{1g} \leftarrow {}^3A_{2g}$ and $^3T_{2g} \leftarrow {}^3A_{2g}$ transitions, respectively, of the Ni^{II} under pseudo octahedral symmetry (Fig. 4).

Complex **1** was converted into **2** by treatment with an equimolar amount of NaOH in water, and **2** was converted into **1** by treatment with acid. Both **1** and **2** are soluble in aqueous NaOH solution (excess NaOH) and show the same absorption spectrum with one visible band at *ca.* 627 nm (ε 320 M^{-1} cm^{-1}) (see insert of Fig. 3). The species existing in alkaline solution must be $[Cu_2(L)_2]^{2-}$ containing the fully-deprotonated ligand L^{3-}, and it may have a *trans* configuration as its visible spectrum is similar to the reflectance spectrum of **1**. The acidification of the alkaline solution resulted in the precipitation of **1**. Thus, the following interconversion is established: *trans*-$[Cu_2(HL)_2]$ (**1**) $\rightleftharpoons$ *cis*-$[Cu_2(HL)(L)]^-$ (**2**) $\rightleftharpoons$ *trans*-$[Cu_2(L)_2]^{2-}$ (see Chart 2, a).

When **3** was treated with an equimolar amount of NaOH in water, about one half of the sample dissolved and the resulting yellowish green solution showed two absorption bands at 620 and 1137 nm. Complex **3** was completely dissolved in an aqueous solution containing excess NaOH to give the same absorption spectrum as observed above (see insert of Fig. 4). The species existing in the alkaline solution must be *trans*-$[Ni_2(L)_2(H_2O)_4]^{2-}$ judging from the marked spectral resemblance to **3**. The acidification of the alkaline solution resulted in the precipitation of **3**. Thus, *cis*/*trans* topology is not the case of the dinuclear Ni complexes (Chart 2, b).

It is of value to consider why *cis* dinuclear Ni species corresponding to **2** cannot exist. The X-ray crystallography for **2′** indicates that the $\{CuN_2O_2\}$ chromophore has moderate Cu–N and Cu–O bond distances (1.943(3)–1.958(2) Å) whereas the $\{CuO_4\}$ chromophore has short Cu–O bond distances (1.883(2)–1.916(2) Å). The N_2O_2 site may accommodate high-spin Ni^{II} by slightly enlarging the cavity, but the O_4 site is too small to accommodate high-spin Ni^{II}. It appears that the O_4 cavity is suitable for low-spin Ni^{II} with a short Ni-to-donor bond distance (< 1.9 Å), but Ni^{II} cannot be of low-spin in the O_4 site because the metal d_π orbitals are destabilized owing to the strong π-antibonding character of the phenolate and carboxylate O atoms.[19]

Physicochemical properties

Complexes **1** and **2** each have a subnormal magnetic moment at room temperature (0.99 and 0.70 μ_B, respectively) suggesting an operation of antiferromagnetic interaction within the molecules. The χ_A *vs.* T curves for **1** and **2** are given in Fig. 5. The magnetic susceptibility for **1** decreased with decreasing temperature to a near plateau value of 50×10^{-6} cm^3 mol^{-1} around 90 K and showed an increase below 50 K. The plateau value corresponds to the temperature-independent paramagnetism[20] arising from the second-order Zeeman effect. Similarly, the magnetic susceptibility of **2** continuously decreased with decreasing temperature to a plateau value of 60×10^{-6} cm^3 mol^{-1} near 110 K and showed an increase below 50 K. The slight increase in magnetic susceptibility at low temperature suggests the presence of paramagnetic impurities. Magnetic simulations were carried out using the Bleaney–Bowers equation[21] involving a correction term for paramagnetic impurities (eqn. (1)):

$$\chi_A = (1 - \rho)\{Ng^2\beta^2/kT\}[1 + \exp(-2J/kT)]^{-1} + \rho(Ng^2\beta^2/4kT) + N\alpha \quad (1)$$

where N is Avogadro's number, β is the Bohr magneton, k is the Boltzmann constant, J is the exchange integral, T is the absolute temperature, $N\alpha$ is the temperature-independent paramagnetism, and ρ is the fraction of paramagnetic impurity. A good magnetic simulation was obtained for **1** with eqn. (1),

View Article Online

Published on 02 October 2001. Downloaded by University of York on 22/10/2014 15:44:31.

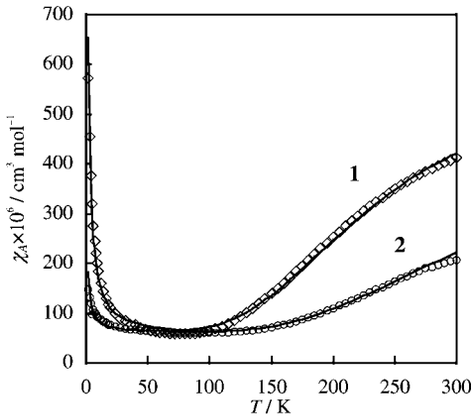

Fig. 5 χ_A *vs.* T curves of **1** and **2**. The solid lines were drawn based on eqn. (1) using the magnetic parameters given in the text.

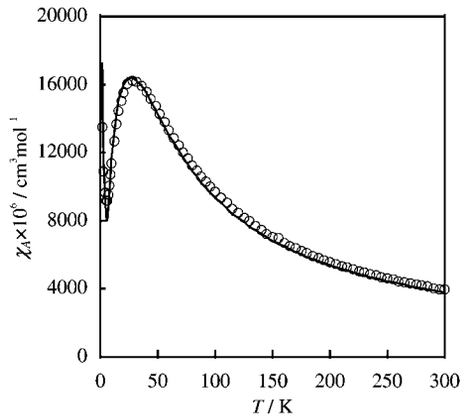

Fig. 6 χ_A *vs.* T curve of **3**. The solid line was drawn based on eqn. (2) using magnetic parameters given in the text.

using magnetic parameters of $g = 2.07$, $J = -255$ cm^{-1}, $Na = 50 \times 10^{-6}$ cm^3 mol^{-1}, and $\rho = 0.003$. The discrepancy factor defined as $R(\chi) = [\Sigma(\chi_{obsd} - \chi_{calcd})^2/\Sigma(\chi_{obsd})^2]^{1/2}$ was 0.053. Similarly, the cryomagnetic property of **2** was well reproduced by eqn. (1), using magnetic parameters of $g = 2.07$, $J = -355$ cm^{-1}, $Na = 60 \times 10^{-6}$ cm^3 mol^{-1}, and $\rho = 0.0006$. The discrepancy factor defined was 0.052.

The χ_A *vs.* T curve of **3** is given in Fig. 6. The magnetic moment at room temperature is 3.07 μ_B which decreased with decreasing temperature to 0.46 μ_B at 2 K. The magnetic susceptibility increased with decreasing temperature to a maximum value at 28 K and then decreased. Such cryomagnetic behavior is typical of a dinuclear Ni(S = 1)Ni(S = 1) system exhibiting an intramolecular antiferromagnetic interaction. The increase in magnetic susceptibility at low temperature indicates the presence of a small amount of paramagnetic impurity. Thus, magnetic simulations for **3** ware carried out using the magnetic susceptibility expression (2)[22] including the correction term for the paramagnetic impurity:

$$\chi_A = (1 - \rho)\{Ng^2\beta^2/kT\}[5 + \exp(-4J/kT)]/[5 + 3\exp(-4J/kT) + \exp(-6J/kT)] + \rho(2Ng^2\beta^2/3kT) + Na \quad (2)$$

The cryomagnetic property of **3** could be well reproduced by this equation using the magnetic parameters, $J = -10$ cm^{-1}, $g = 2.12$, $Na = 300 \times 10^{-6}$ cm^3 mol^{-1} and $\rho = 0.03$. The discrepancy factor for the magnetic simulation was 0.056.

Extension to a pentanuclear system

Complex **2** is of particular interest to us because it has a dioximate group capable of acting as a bridge to a second metal ion. In this study **2** was reacted with Mn^{II} in DMF to obtain $[Mn\{Cu_2(HL)(L)\}_2(H_2O)_4]\cdot H_2O\cdot 2DMF$ (**4**). An ORTEP view of $[Mn\{Cu_2(HL)(L)\}_2(H_2O)_4]\cdot 4H_2O\cdot 2DMF$ (**4′**) is shown in Fig. 7 together with the atom numbering scheme. Selected bond distances and angles are given in Table 4.

The X-ray crystallographic results demonstrate that a linear pentanuclear structure has been formed by the coordination of two $\{Cu_2(HL)(L)\}^-$ molecules to Mn^{II} through one outer carboxylate oxygen. An inversion center exists at the Mn atom. Each $\{Cu_2(HL)(L)\}^-$ unit retains the geometric features found for **2′** except that the axial donor on Cu1 is an aqua oxygen in **2′** but a carboxylate oxygen (O8^a) from an adjacent molecule in **4′** (Cu1–O8^a 2.403(3) Å). Furthermore, Cu2 in the O_4 site in **4′** has a square-pyramidal geometry with the coordination of the oximate oxygen O5^b of an adjacent molecule (Cu2–O5^b 2.457(3) Å). The geometry about the Mn atom is pseudo octahedral with four water molecules on the equatorial base and two carboxylate oxygen atoms at the axial sites. The equatorial Mn–O9 and Mn–O10 bond distances are 2.193(3) and 2.155(3) Å, respectively. The axial Mn–O4 bond distance is significantly elongated (2.248(3) Å). The carboxylate O8^a bound to Cu1 and the oxime oxygen O5^b bound to Cu2 are situated *trans* to each other with respect to the mean molecular plane. As a result, **4′** has a two-dimensional network structure extended in the *ac*

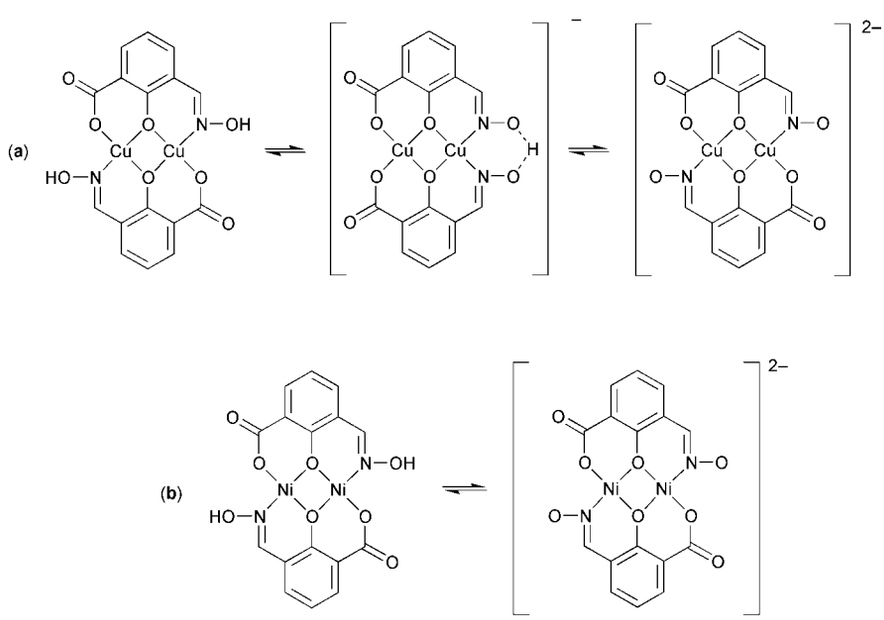

Chart 2 Structural changes of (a) dinuclear Cu complexes and (b) dinuclear Ni complexes.

View Article Online

Published on 02 October 2001. Downloaded by University of York on 22/10/2014 15:44:31.

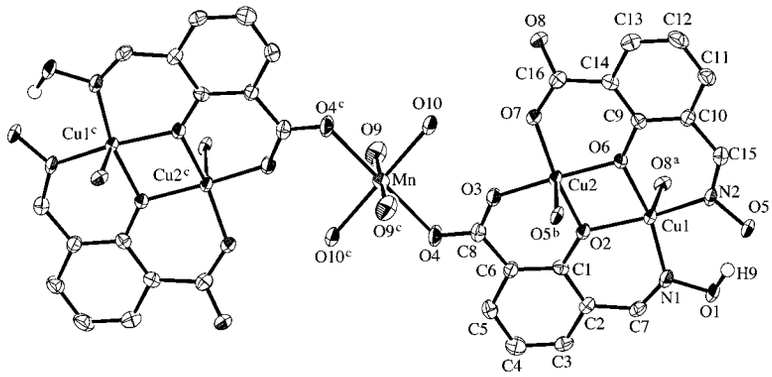

Fig. 7 An ORTEP view of $[Mn\{Cu_2(HL)(L)\}_2(H_2O)_4]\cdot 4H_2O\cdot 2DMF$ (**4′**) with the atom numbering scheme.

Table 4 Selected bond distances (Å) and angles (°) for **4′**

Cu(1)–O(2)	1.960(3)	Cu(2)–O(2)	1.923(3)
Cu(1)–O(6)	1.948(3)	Cu(2)–O(3)	1.875(3)
Cu(1)–O(8^a)	2.403(3)	Cu(2)–O(5^b)	2.457(3)
Cu(1)–N(1)	1.936(3)	Cu(2)–O(6)	1.914(3)
Cu(1)–N(2)	1.946(3)	Cu(2)–O(7)	1.897(3)
Mn–O(4)	2.248(3)	Mn–O(9)	2.193(3)
Mn–O(10)	2.155(3)	Cu(1)···Cu(2)	2.991(1)
Cu(2)···Mn	5.025(1)	Cu(1)···Mn	7.729(1)
O(2)–Cu(1)–O(6)	77.8(1)	O(2)–Cu(2)–O(3)	94.1(1)
O(2)–Cu(1)–O(8^a)	97.6(1)	O(2)–Cu(2)–O(5^b)	93.8(1)
O(2)–Cu(1)–N(1)	90.3(1)	O(2)–Cu(2)–O(6)	79.5(1)
O(6)–Cu(1)–O(8^a)	95.80(10)	O(3)–Cu(2)–O(5^b)	93.3(1)
O(6)–Cu(1)–N(2)	90.2(1)	O(3)–Cu(2)–O(7)	90.3(1)
O(8^a)–Cu(1)–N(1)	89.4(1)	O(5^b)–Cu(2)–O(6)	93.8(1)
O(8^a)–Cu(1)–N(2)	95.3(1)	O(5^b)–Cu(2)–O(7)	99.8(1)
N(1)–Cu(1)–N(2)	100.6(1)	O(6)–Cu(2)–O(7)	94.4(1)
Cu(1)–O(2)–Cu(2)	100.8(1)	Cu(1)–O(6)–Cu(2)	101.5(1)
O(4)–Mn–O(9)	94.5(1)	O(4)–Mn–O(9^c)	85.5(1)
O(4)–Mn–O(10)	96.7(1)	O(4)–Mn–O(10^c)	83.3(1)
O(9)–Mn–O(10)	89.3(1)	O(9)–Mn–O(10^c)	90.7(1)

Symmetry operations: ^{a} $-x, -y + 1, -z + 1$. ^{b} $-x, -y + 1, -z$. ^{c} $-x, -y, -z + 1$.

plane. The four lattice water molecules are hydrogen-bonded to the complex molecule through the oxime oxygen atom O5 (O5^c) (O5···O 2.883(5) Å) and between the carboxylate oxygen atom O8 (O8^c) and the hydrogen attached to O10 (O10^c) (O8···O 2.803(4); O10···O: 2.715(4) Å). The two DMF molecules are also involved in hydrogen bonding to the hydrogen attached to O9 (O9^c) (O9···O(DMF): 2.657(4) Å).

Complex **4** has a room-temperature magnetic moment of 6.32 μ_B that decreased with decreasing temperature to 5.58 μ_B at 2 K. Evidently an antiferromagnetic interaction operates between the adjacent Cu^{II} and Mn^{II} ions through the carboxylate group, but it must be emphasized that the magnetic moment at 2 K is significantly low for $S_T = 5/2$ arising from an antiferromagnetic interaction within the pentanuclear CuCuMnCuCu unit. It appears that an intermolecular antiferromagnetic interaction also occurs between the adjacent pentanuclear units, probably through the Cu2–O5^b–N2^b–Cu1^b pathway.

Contrary to expectation, the pentanuclear core of **4** is extended by the carboxylate group but not the dioximate group. This may relate to the strong hydrogen bond in the N–O···H···O–N linkage. Further attempts for providing dioximate-bridged polynuclear metal complexes using **2** are under way.

Acknowledgements

This work was supported by a Grant-in-Aid for COE Research 'Design and Control of Advanced Molecular Assembly System' from the Ministry of Education, Science and Culture, Japan (No. 08CE2005).

References

1 A. Chakravorty, *Coord. Chem. Rev.*, 1974, **13**, 1.
2 D. Luneau, H. Oshio, H. Ōkawa and S. Kida, *Chem. Lett.*, 1989, 443; H. Ōkawa, M. Koikawa, S. Kida, D. Luneau and H. Oshio, *J. Chem. Soc., Dalton Trans.*, 1990, 469; D. Luneau, H. Oshio, H. Ōkawa, M. Koikawa and S. Kida, *Bull. Chem. Soc. Jpn.*, 1990, **63**, 2212; D. Luneau, H. Oshio, H. Ōkawa and S. Kida, *J. Chem. Soc., Dalton Trans.*, 1990, 2282.
3 C. B. Singh and B. Sahoo, *J. Inorg. Nucl. Chem.*, 1974, **36**, 1259.
4 Z. J. Zhong, H. Ōkawa, N. Matsumoto, H. Sakiyama and S. Kida, *J. Chem. Soc., Dalton Trans.*, 1991, 497.
5 R. Ruiz, M. Julve, J. Faus, F. Lloret, M. C. Muñoz, Y. Journaux and C. Bois, *Inorg. Chem.*, 1997, **36**, 3434.
6 E. Colacio, J. M. Dominguez-Vera, A. Escuer, R. Kivekäs and A. Romerosa, *Inorg. Chem.*, 1994, **33**, 3914.
7 C. Krebs, M. Winter, T. Weyhermuller, E. Bill, K. Wieghardt and P. Chaudhuri, *J. Chem. Soc., Chem. Commun.*, 1995, 1913.
8 C. N. Verani, E. Rentschler, T. Weyhermuller, E. Bill and P. Chaudhuri, *J. Chem. Soc., Dalton Trans.*, 2000, 251.
9 N. Fukita, M. Ohba and H. Ōkawa, *J. Chem. Soc., Dalton Trans.*, 2000, 64.
10 H. Ōkawa, I. Hanaoka and S. Kida, *Chem. Lett.*, 1974, 71.
11 M. Tanaka, H. Ōkawa, T. Tamura and S. Kida, *Bull. Chem. Soc. Jpn.*, 1974, **47**, 1669.
12 *Landolt-Börnstein*, Neue Series II/11, Springer-Verlag, Berlin, 1981.
13 J. C. Duff and E. J. Bills, *J. Chem. Soc.*, 1932, 1987.
14 TEXSAN, Molecular Structure Analysis Package, Molecular Structure Corporation, Houston, TX, 1985 and 1992.
15 C. K. Johnson, ORTEP, Report 3794, Oak Ridge National Laboratory, Oak Ridge, TN, 1965.
16 E. Frasson, R. Bardi and S. Bezzi, *Acta Crystallogr.*, 1959, **12**, 201.
17 L. E. Godycki and R. E. Rundle, *Acta Crystallogr.*, 1953, **6**, 487.
18 R. E. Rundle and M. Parasol, *J. Chem. Phys.*, 1952, **20**, 1487.
19 H. Ōkawa and D. H. Busch, *Inorg. Chem.*, 1979, **18**, 1555.
20 B. N. Figgis and J. Lewis, *Prog. Inorg. Chem.*, 1964, **6**, 37.
21 B. Bleaney and K. D. Bowers, *Proc. R. Soc. London, Ser. A*, 1952, **214**, 451.
22 J. A. Andrew, P. W. Ball and A. B. Blake, *J. Chem. Soc. A*, 1969, 1408.